VEKSLER AND BALDIN LABORATORY OF HIGH ENERGIES

In 2006 the scientific programme of the Veksler and Baldin Laboratory of High Energies (VBLHE), Joint Institute for Nuclear Research (JINR), as in the previous years, was concentrated on investigations of interactions of relativistic nuclei in the energy range between a few hundred MeV and a few TeV per nucleon to search for manifestations of quark and gluon degrees of freedom in nuclei, asymptotic laws of nuclear matter in high energy collisions, as well as on the study of the spin structure of the lightest nuclei.

Experiments along these lines were carried out with the beams of the VBLHE accelerator complex as well as accelerators at CERN, BNL, GSI, and others. Today VBLHE is an accelerator centre at which a wide range of research is feasible in the energy region where the transition from the effects of the nucleon structure of a nucleus to the asymptotic behavior in nuclear interactions takes place. International scientific cooperation of the Laboratory is diverse: CERN, many physics centres in Russia, scientific centres in the JINR Member States, a number of research centres in the USA, Germany, France, Japan, and other countries.

New results were obtained in design of tests of the superconducting fast-cycling and fast ramped magnets and cables aimed for SIS100 at GSI. The data obtained can also be useful for the future LHC booster upgrade.

The total running time of the Nuclotron is 1101 hours.

BECQUEREL Collaboration

In the peripheral fragmentation of a relativistic nucleus with charge Z the ionization induced by the fragments can decrease down to a factor Z; while the ionization per one track, down to Z^2. Therefore, experiment should provide an adequate detection range. In order to reconstruct an event, complete kinematic information about the particles in the relativistic fragmentation cone is needed which, e.g., allows one to calculate the invariant mass of the system. The accuracy of its estimation decisively depends on the exactness of the track angular resolution. To ensure the best angular resolution, it is necessary that the detection of relativistic fragments should be performed with the best spatial resolution.

The nuclear track emulsion technique, which underlies the BECQUEREL project at the JINR Nuclotron, well satisfies the above-mentioned requirements [1–9]. It is aimed at a systematic search for peripheral fragmentation modes with statistical provision at a level of dozens of events, their classification and angular metrology. Emulsions provide a record special resolution (about 0.5 μm) which allows one to separate the charged particle tracks in the three-dimensional image of an event within one-layer thickness (600 μm) and ensure a high accuracy of angle measurements.

Fragmentation of ^{14}N Nuclei. A stack of layers of BR-2 emulsion was exposed to a beam of ^{14}N nuclei accelerated to a momentum of $2.86A$ GeV/c at the JINR Nuclotron [6]. The charge topology distribution of ^{14}N peripheral interactions indicates the leading role of the $2+2+2+1$ charge configuration channel. In order to estimate the energy scale of production of 3α particle systems in the $^{14}\mathrm{N} \rightarrow 3\alpha + X$ channel, the invariant excitation energy Q distribution with respect to the ^{12}C ground state has been obtained (Fig. 1). The main part of the events is concentrated in the Q area from 10 to 14 MeV, covering the known ^{12}C levels. To estimate the fraction of the events involving the production of an intermediate ^{8}Be nucleus in the reactions $^{14}\mathrm{N} \rightarrow {}^8\mathrm{Be} + \alpha + X$ the invariant excitation energy distribution for an α-particle pair with respect to the ^{8}Be ground state has been obtained (Fig. 2). The first distribution peak relates to the value to be expected for the decay products of an unstable ^{8}Be nucleus in the ground state 0^+. This part of the spectrum increased by a factor of 20 is presented in the inset. The distribution centre is seen to coincide well with the decay energy of the ^{8}Be ground state. The fraction of the α particles originating from the ^{8}Be decay is 25–30%.

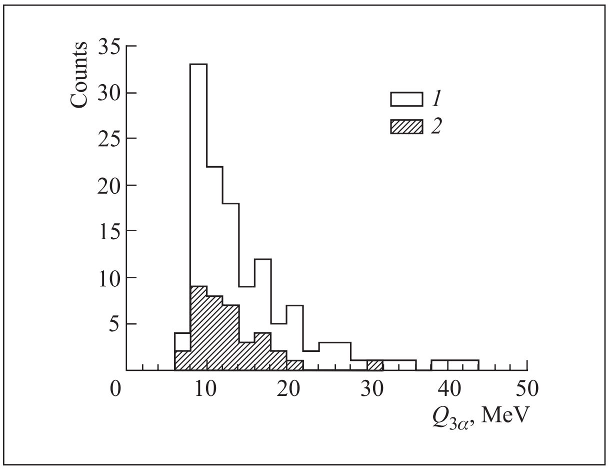

Fig. 1. The invariant excitation energy Q_α distribution of three α particles with respect to the ^{12}C ground state for the process $^{14}\mathrm{N} \to 3\alpha + X$ (*1* — all the events of the given dissociation, *2* — «white» stars)

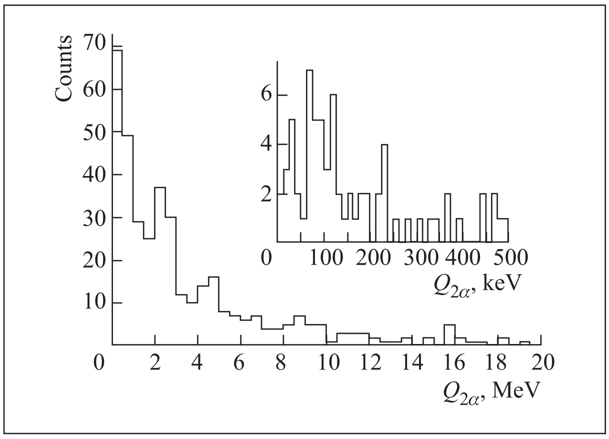

Fig. 2. The invariant excitation energy $Q_{2\alpha}$ distribution of α-particle pairs for the process $^4\mathrm{N} \to 3\alpha + X$. In the inset: a fraction of the distribution at 0–500 keV

Fragmentation of ^{7}Be Nuclei. Nuclei of ^{7}Li were accelerated at the JINR Nuclotron. After the charge-exchange reaction involving these nuclei at an external target a second ^{7}Be beam of energy $1.2A$ GeV was formed. This beam was used to expose photo-emulsion chambers [8]. The mean free path for inelastic ^{7}Be interactions in emulsion $\lambda_{\mathrm{inel}}(^7\mathrm{Be}) = (14.0 \pm 0.8)$ cm coincides within the errors with those for ^{6}Li and ^{7}Li nuclei. More than 10% of the ^{7}Be events are associated with the peripheral interactions in which the total charge of the relativistic fragments is equal to the charge of the ^{7}Be and in which charged mesons are not produced. An unusual ratio of the stable isotopes is revealed in the composition of the doubly charged ^{7}Be fragments — the number of ^{3}He fragments is twice as large as that of ^{4}He fragments. In 50% of peripheral interactions, a ^{7}Be nucleus decays to two doubly charged fragments. In 50% of events, the ^{7}Be fragmentation proceeds only to charged fragments involving no emission of neutrons. Of them, the $^3\mathrm{He} + {}^4\mathrm{He}$ channel dominates, while the $^4\mathrm{He} + d + p$ and $^6\mathrm{Li} + p$ channels constitute 10% each. Two events involving no emission of neutrons are registered in the three-body $^3\mathrm{He} + t + p$ and $^3\mathrm{He} + d + d$ channels. The particular features of the relativistic ^{7}Be fragmentation in such peripheral interactions are explained by the $^3\mathrm{He} + {}^4\mathrm{He}$ two-cluster structure of the ^{7}Be nucleus.

Peripheral Fragmentation of ^{8}B Nuclei. For the first time, nuclear emulsions were exposed to a beam of radioactive ^{8}B nuclei [9]. Detailed data have been obtained on the probabilities of the ^{8}B fragmentation channels in peripheral interactions at $1.2A$ GeV. A leading contribution of the $^8\mathrm{B} \to {}^7\mathrm{Be} + p$ mode having the lowest energy threshold was revealed. Information about a relative probability of dissociation modes with larger multiplicity has been obtained. The ^{7}Be core dissociation in ^{8}B is found to be similar to that of the free ^{7}Be nucleus. A further analysis of the fragmentation topology suggests the identification of the H and He isotopes.

The transverse momentum distributions for the $^8\mathrm{B} \to {}^7\mathrm{Be} + p$ dissociation fragments have been obtained (Fig. 3). Their small average value, $\langle P_T^* \rangle = (52 \pm 5)$ MeV/c, in the c.m.s. reflects a low binding energy of the external proton in the ^{8}B nucleus. In the selection of the events in which a transverse momentum of less than 60 MeV/c is transferred to the ^{8}B nucleus, there appears a strong azimuthal angle correlation between ^{7}Be and p.

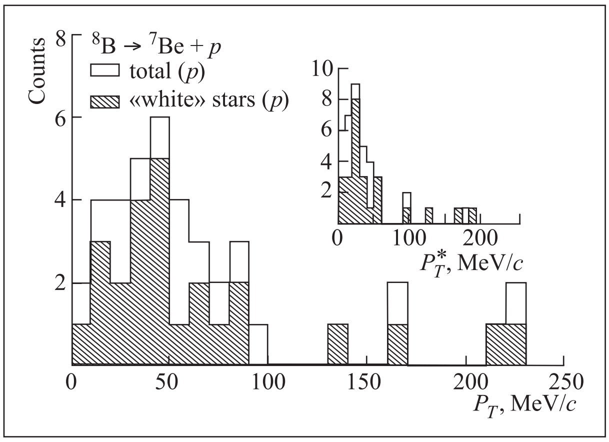

Fig. 3. The P_T transverse momentum distribution of the protons produced in peripheral stars $^8\mathrm{B} \to {}^7\mathrm{Be} + p$. In the insertion the same distribution is given in the c.m.s. of $^7\mathrm{Be} + p$

FASA Collaboration

The existence of the spinodal region for the hot nuclear matter was predicted more than 30 years ago. The nuclear rigidity is equal to zero on the border of this region: $\partial p / \partial V = 0$. The experimental information about the spinodal state of nuclear matter is gained by studies of the process of nuclear multifragmentation. The FASA collaboration made a remarkable contribution in this field [10].

The spinodal decomposition associates with the *liquid–fog* phase transition in a nuclear system rather than with the *liquid–gas* transition. This scenario is evidenced by the following observations made by a number of collaborations, and FASA too:

• Density of the system at the breakup is 2–3 times smaller than the normal one ρ_0 [11].

• The lifetime of the fragmenting system is very small, $\sim 2 \cdot 10^{-22}$ s (or ≈ 70 fm/c). It was measured for the first time in Dubna (1994) by analysis of IMF–IMF angular correlations [12].

• The breakup temperature ($T = 4{-}6$ MeV) is lower than the critical temperature for the *liquid–gas* phase transition, which is found by FASA to be $T_c = (17 \pm 2)$ MeV.

The last point is crucial for the statement about observation of the spinodal state of nuclear matter. Therefore, this year a new and more refined analysis of the data was done to get more reliable value of the critical temperature and breakup volume (see Figs. 4 and 5) [13]. It is found that $T_c \geqslant 18$ MeV and $V_t/V_0 = 3$ (or $\rho_t = 1/3\rho_0$).

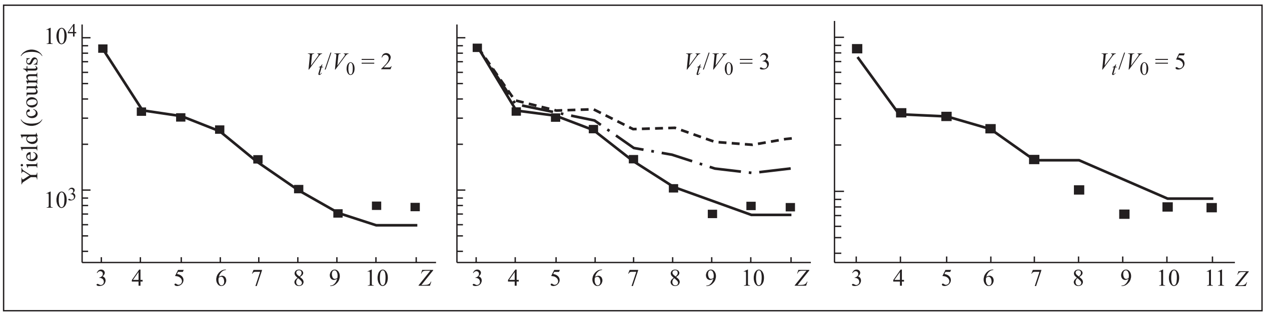

Fig. 4. The IMF charge distributions for $p\,(8.1$ GeV$)+$Au collisions. Symbols: measured IMF charge distributions. Solid lines: calculated IMF charge distributions assuming $T_c = 18$ MeV and breakup volumes indicated. Dashed and dot-dashed lines: calculated IMF charge distributions for $T_c = 7$ and 11 MeV

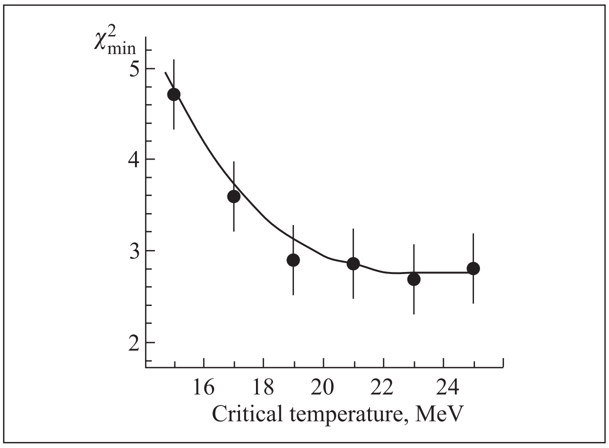

Fig. 5. The minimal values of χ^2as a function of the critical temperature

The modernization of the FASA setup has been accomplished. We have got FASA-3, which is supplied by a new detector array. It consists of 25 closely packed telescopes $dE(\mathrm{gas}) \times E(\mathrm{Si})$. The detector was created in the H. Niewodniczanski Institute (Cracow). It gives the possibility to measure the IMF–IMF correlation both in respect to relative angle and to relative velocity with selection of fragments by charge and energy. The further experimental studies are of the great interest to get more information on the properties of the spinodal state of nuclear matter.

MARUSYA Collaboration

The main objective of measurements was the investigation of the spectra of pions, protons and kaons in nuclear interactions with extracted beams of the Nuclotron.

Measurements were performed using carbon beams with an energy of 2.2 GeV/nucleon using small-size Cu targets (4×4 mm). Particles produced in interactions (π, K, p) with momenta of 500, 1500 MeV/c were registered at an angle of 30° with the angular spread 1–2°. The main methodical purpose of measurements was adjustment and study of modes of operation of the magneto-optical spectrometer on the basis of the focal factor method using the new hodoscope detector placed in close vicinity of the target.

During measurements, experimental estimates of a possibility of registration and identification of two particles in one event with close momenta and traveling at the same angle (within the angle of registration 2–3° of the magneto-optical spectrometer). Measurements demonstrated a possibility of registration of such events with sufficient statistical confidence (up to 100 events per hour) for investigation of the effective mass spectrum for states produced via the channels (πK, πp, Kp, pp, $\pi\pi$). Special attention was paid to the reaction $A + A \to K^+p$ in the region of effective masses 1500 MeV in regard to the interest in investigation of possible states called pentaquarks.

Figure 6 shows the time-of-flight spectra for three modes of operation of the spectrometer obtained in this run in the reaction C + Cu. For identification of kaons an additional multifactor analysis of the obtained data is required. This analysis is being performed at present.

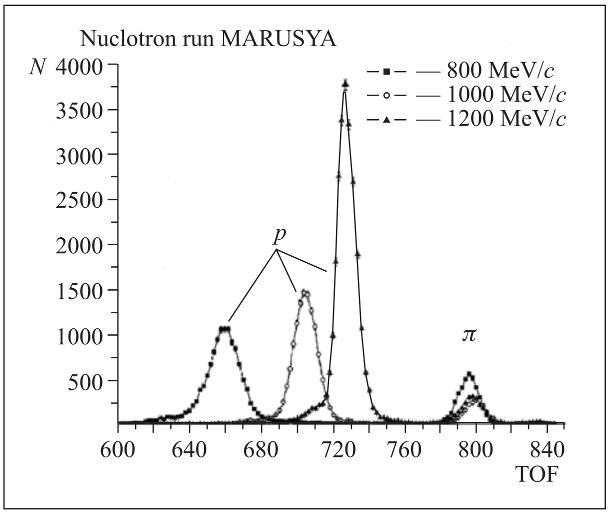

Fig. 6. Time-of-flight spectra of protons and pions obtained in the reaction C + Cu for three momenta of the registered particles

Figure 7 shows the coordinate profiles of the beam for two modes of operation of the magnets SP-40, SP-57 for the fixed mode of operation of the magnetic lenses. These profiles were obtained on the basis of the measured times of particle registration from the edges of the detector.

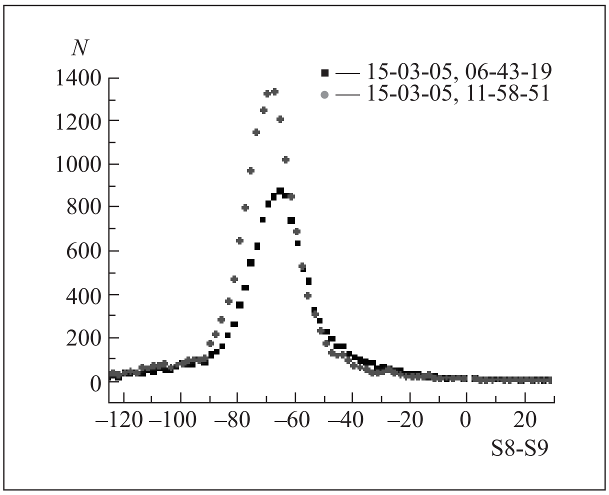

Fig. 7. Coordinate profiles of the beam for two modes of operation of the magnets SP-40, SP-57 for the fixed mode of operation of the magnetic lenses

Figure 8 shows the coordinate profiles of the beams for determination of the optimal capture of the given momentum by the magnets of the spectrometer when the lenses are switched off.

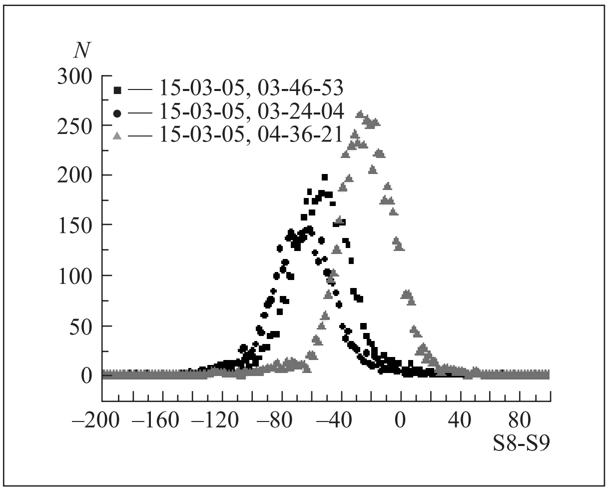

Fig. 8. Coordinate profiles of the beams for determination of the optimal capture of the given momentum by the magnets of the spectrometer when the lenses are switched off

The obtained set of data in the whole range of operation of the magnetic elements of the MARUSYA spectrometer demonstrated a possibility of precision adjustment of the spectrometer without special coordinate detectors. The physical information on the ratios of the pion, kaon and proton yields will be analyzed when the time-of-flight and amplitude spectra obtained during measurements are processed.

First Observation of the Parametric X-ray Radiation from Moderately Relativistic Nuclei in Crystals

The main purpose of the experiment «Crystal» was observation and investigation of parametric X-ray radiation (PXR) from relativistic nuclei in a tungsten crystal, which has another, different from silicon, type of crystallographic lattice [14].

Besides, the experiment was performed in a new Laue geometry when the X-ray detector registers radiation from a crystal plate surface, which is opposite to the incident beam.

It is necessary to note that a unique situation is realized at the beam of nuclei with energy of the order of 1 GeV per nucleon when a formation of parametric radiation from particles in a crystal occurs by a few families of crystallographic planes simultaneously. This occurs due to a wide angular distribution of the virtual photon field of incident nuclei (the distribution width is inversely proportional to the relativistic factor of particles).

This situation cannot be realized at the electron beams. Electrons with a small value of relativistic factor have trajectories in the crystals which are different from straight lines. This breaks conditions for the parametric radiation formation.

The experiment was performed at the Nuclotron beam of carbon nuclei with an energy of 2 GeV per nucleon using tungsten crystals. The crystal was installed perpendicularly to the beam. In this case, the X-ray radiation with the same wavelength has to be formed at different families of crystallographic planes for a fixed direction of observation.

Figure 9 shows the spectra measured with (111) and (110) tungsten crystals (*a* and *b*, correspondingly). The maximum noted as W, L_γ is formed by photons of the characteristic radiation generated by particles in a tungsten crystal. The maxima E_γ correspond to calculated positions of parametric radiation lines for the Laue experiment geometry. The PXR maximum for the (110) tungsten crystal is wider than for the (110) case. A greater dimension of irradiated crystal area, which gives a greater interval of the PXR observation angles, can cause it.

A possibility in a future experiment to have an intensive beam, which is narrow in the observation plane, will allow observing narrower and well-formed maxima of PXR.

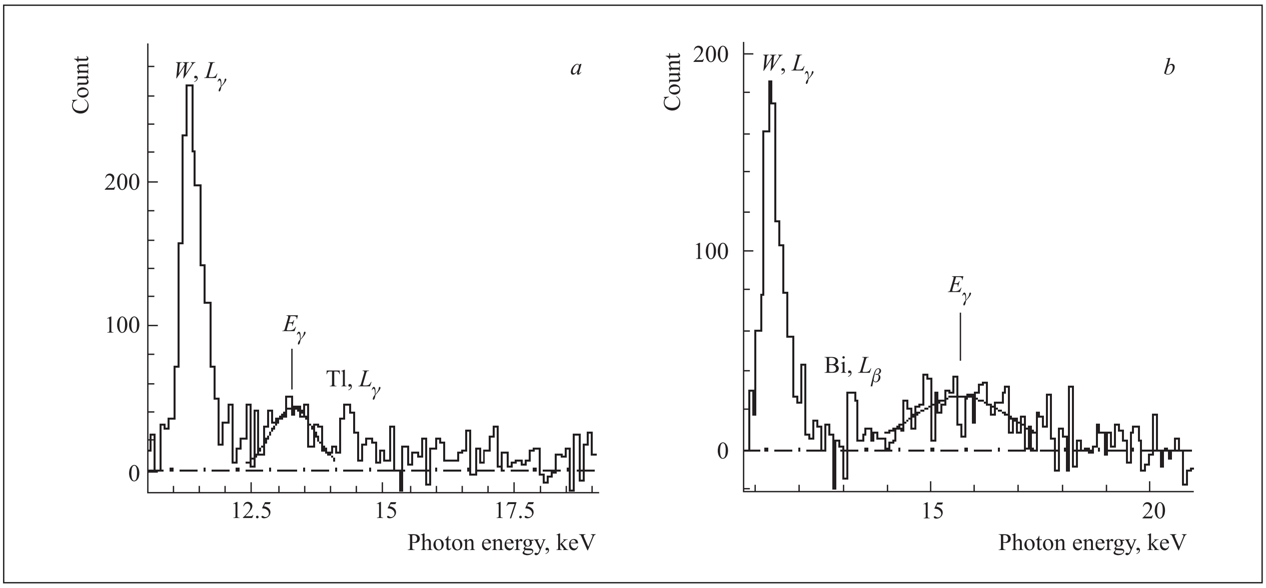

Fig. 9. The spectra measured with (111) and (110) tungsten crystals (*a* and *b*, correspondingly)

Construction and Testing of the ALICE TRD Chambers

The ALICE experiment is designed for the study of the physics of strongly interacting matter and quark–gluon plasma in nucleus–nucleus collisions in the new large hadronic collider (LHC) at CERN [15]. Transitional radiation detector (TRD) is one of the major components of the ALICE setup. The main task of TRD is electron identification with a high efficiency and the work-out of trigger signal for the electrons with a high transverse momentum [16]. TRD consists of 540 wire chambers (12 types of size). The total sensitive area of the detector is ~ 736 m^2, the number of electronics channels is about 1.2 million [17]. Mass production of TRD chambers was started in 2005 at JINR, Universities of Heidelberg and Frankfurt, GSI (Darmstadt), and NIPNE (Bucharest). For TRD chambers construction and testing, at the Laboratory of High Energies a new detector laboratory was equipped with the «clean» rooms of total area ~ 120 m^2.

The wire plane at TRD chambers is placed with a precision of ~ 20 microns. During the production the chambers are tested on the computer control test stand equipped with an X-ray tube, which can move with a high accuracy in X/Y directions and makes it possible to scan the full area of the chamber.

Constructed and tested TRD chambers are shipped to GSI (Darmstadt), where they are assembled with FEE and readout electronics. Ninety chambers have been constructed at VBLHE by the end of 2006. Sixty-five chambers were shipped to Germany to be additionally tested and prepared for the assembling to 18 TRD Supermodules [18].

ALICE Collaboration

In 2006 a very large dipole magnet for the muon spectrometer was assembled and tested at full current in the operation position. The field was measured.

674 lead tungstate crystals were tested at JINR setup and certified for optical properties. JINR group took part in tests of the first fully assembled module of the PHOS spectrometer at PS beam at CERN. Analysis of test beam data was performed. An improved algorithm for the π^0 identification at energies more than 40 GeV

was developed. It was based on results of 256-channel prototype testing at SPS beam.

The part of the Physics Performance Report HBT section on the resonance influence for the HBT was prepared. A study of vector meson decays to di-electron in the ALICE for Pb–Pb interactions was done. More detailed study of the heavy quarkonia production in collisions of proton with lead nuclei and of lead nuclei with proton at the muon spectrometer of ALICE has been performed. The Universal Hydro-Kinetic Model (UHKM) was finished as the Monte-Carlo code for special study of HBT correlations. The model describes the HBT radii from SPS and RHIC experiments. A special version of model with parameters tuning for LHC energy has been created.

Comparison of the energy and space resolution simulation in the PHOS spectrometer in the framework of the GEANT3 and FLUKA transport codes within ALIROOT was done. Cluster finder & tracking on the basis of Kalman filter method developed by JINR team has been committed in ALIROOT as default option for the reconstruction in the muon spectrometer. The update of the PHOS calorimeter geometry in ALIROOT has been done, strip alignment in PHOS modules is under installation into ALIROOT. The common viewer architecture used by all 3D viewers has been developed and applied. Organizational and technical management of Russian computer centres in the Data Challenge of ALICE 2006 and Services Challenge4 was provided. Generation and reconstruction of pp and Pb–Pb events for ALICE was successfully processed by eight Russian sites together with JINR site based on LCG resources.

HADES Project (JINR Participation)

In 2006 JINR team participated in production beam time of May 3–16 ($p+p$ @ 1.25 GeV). More than 10^9 events were collected with 1st and 2nd levels trigger, data analysis is in progress. JINR team took an active part in the data analysis and development of tracking software, as well as of the software for the drift chambers alignment. The new electronics modules were developed at JINR for drift chambers which will be used for 3rd level trigger.

The article of the HADES collaboration «Dielectron Production in $^{12}\mathrm{C}+^{12}\mathrm{C}$ Collisions at $2A$ GeV with the HADES Spectrometer» was published in the journal «Physical Review Letters» [19]. 3D HADES Spectrometer view was published in an article of the German magazine «Bild der Wissenschaft» dedicated to high level research in nuclear physics [20].

The physical programme for systematic studies of dilepton production in heavy-ion collisions at energies between 1 and $10A$ GeV with HADES spectrometer is under development. Appropriate EU fund (FP-6) was taken for the HADES upgrade (for RPC and Forward Wall TOF).

LNS–pHe3 Collaboration

The experimental results on the tensor analyzing power T_{20} for $\vec{d}^{12}\mathrm{C} \to p^{13}\mathrm{C}$ and $\vec{d}d \to p^3\mathrm{H}$ reactions at energy $T_d = 140$, 200 and 270 MeV at emission angle $\Theta_{\mathrm{cm}} = 0°$ from R308n experiment at RIKEN are presented. The $\vec{d}d \to pX$ data near breakup threshold are presented too. The experimental results on the tensor analyzing power T_{20} for $\vec{d}^{12}\mathrm{C} \to p^{13}\mathrm{C}^*$ reactions with excitation of levels of a nucleus $^{13}\mathrm{C}$ at energy $T_d = 140$, 200 and 270 MeV at emission angle $\Theta_{\mathrm{cm}} = 0°$ are also obtained.

The interest in the experimental and theoretical study of few nucleon transfer reactions has been renewed in the past years mainly due to the possibility to obtain information of astrophysical relevance from these reactions. Direct measurement of capture reactions at energies of astrophysical interest is, in some cases, nearly impossible due to the low reaction yield, especially if the capture involves exotic nuclei. Alternative indirect methods, such as the asymptotic normalization coefficient (ANC) method, based on the analysis of breakup or transfer reactions, have been used as a tool to obtain astrophysical S factors. The advantage of indirect approaches comes from the fact that transfer and breakup reactions can be measured at higher energies, where the cross-sections are much larger.

Experimental results for the tensor analyzing power T_{20} for $\vec{d}^{12}\mathrm{C} \to pX$ and $\vec{d}d \to pX$ reactions at energy $T_d = 140$, 200 and 27 MeV at emission angle $\Theta_{\mathrm{cm}} = 0°$ are presented in Figs. 10–12. The systematic error due to uncertainty in the beam polarization and statistical error are added in quadrature.

The ONE calculations predict that the tensor analyzing power at the forward angles is sensitive to the structure $^3\mathrm{H}$.

The filled stars are the results of the tensor analyzing power T_{20} for $\vec{d}d \to p^3\mathrm{H}$ reaction at energy $T_d = 140$, 200 and 270 MeV (Fig. 10). The experimental data on tensor analyzing power T_{20} for $\vec{d}d \to pX$ are presented by the filled symbols. Open symbols correspond to the data for $\vec{d}^{12}\mathrm{C} \to pX$ reaction.

The data taking was performed chronologically at 270, 200 and 140 MeV. The intensity of polarized deuteron beam was decreased because of ageing of polarized ion source.

The experimental data on tensor analyzing power T_{20} for $\vec{d}d \to p^3\mathrm{H}$ reactions (solid circles), for $\vec{d}d \to pdn$ reactions (square symbols) and for $\vec{d}d \to ppnn$ reactions (triangular symbols) are shown in Fig. 11. The comparison of these polarization observables for the breakup reactions ($\vec{d}(d,p)\,dn$ and $\vec{d}(d,p)\,pnn$) gives an opportunity to conclude that they are in an agreement within achieved experimental errors.

The results for the tensor analyzing power T_{20} for $\vec{d}^{12}\mathrm{C} \to p^{13}\mathrm{C}_{\mathrm{g.s.}}$ reactions (solid circles), for $\vec{d}^{12}\mathrm{C} \to p^{13}\mathrm{C}^*(3.089)$ reactions (square symbols) and for $\vec{d}^{12}C \to p^{13}C^*(3.6845 + 3.854)$ (triangular symbols) are presented in Fig. 12. The behavior of T_{20} for $\vec{d}^{12}C \to pX$ reactions is not clear from Fig. 12. Studying of polarizing observable T_{20} in wider energetic region is necessary for understanding its behavior.

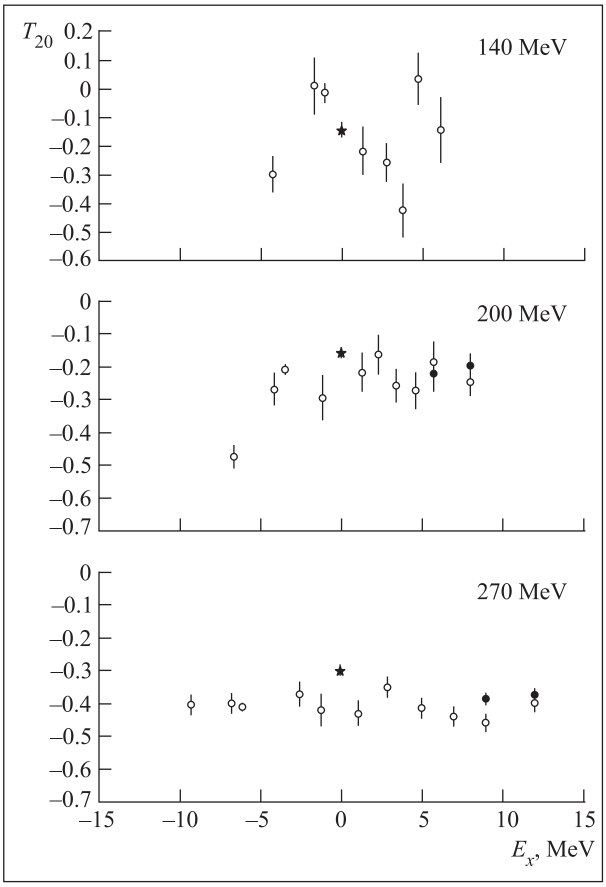

Fig. 10. The experimental results of T_{20} analyzing powers for $\vec{d}^{12}C \to pX$ and $\vec{d}d \to pX$ reactions at energy $T_d = 140$, 200 and 270 MeV at emission angle $\Theta_{cm} = 0°$ depending on E_x

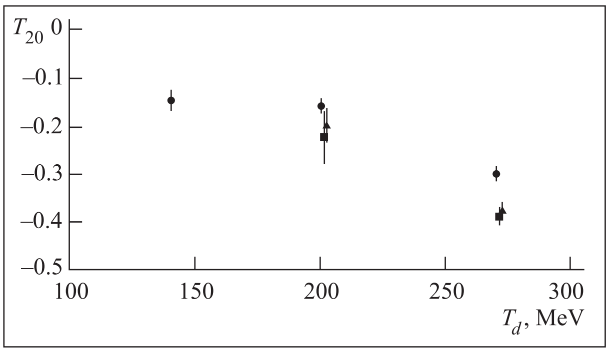

Fig. 11. The experimental results of T_{20} analyzing powers for $\vec{d}d \to pX$ reactions at energy $T_d = 140$, 200 and 270 MeV at emission angle $\Theta_{cm} = 0°$

The tensor analyzing power T_{20} for $\vec{d}^{12}C \to pX$ and $\vec{d}d \to pX$ reactions at energy $T_d = 140$, 200 and 270 MeV at emission angle $\Theta_{cm} = 0°$ has negative sign. The energy dependence of T_{20} demonstrates the decreasing of T_{20} magnitude with the energy. This behavior can be understood in terms of D/S wave ratio in the ^3H, ^{13}C with the help of ONE.

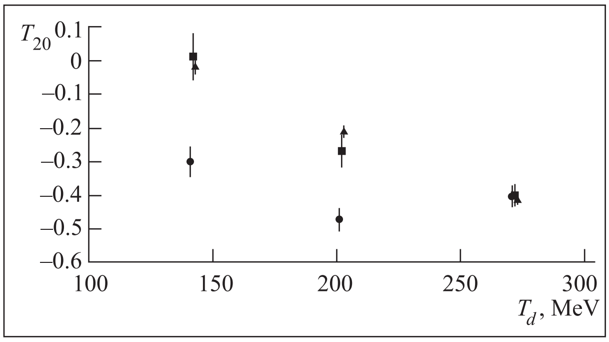

Fig. 12. The experimental results of T_{20} analyzing powers for $\vec{d}^{12}C \to pX$ reaction at energy $T_d = 140$, 200 and 270 MeV at emission angle $\Theta_{cm} = 0°$

The results for the tensor analyzing power T_{20} for $\vec{d}^{12}C \to pX$ and $\vec{d}d \to pX$ reactions at energy $T_d = 140$, 200 and 270 MeV have been obtained.

The experimental data on T_{20} for these reactions show sensitivity to the spin structure of deuteron.

The negative sign of the analyzing power T_{20} for $\vec{d}^{12}C \to pX$ and $\vec{d}d \to pX$ reactions also reflects D/S ratio a components of wave function of deuteron.

The tensor analyzing power T_{20} has negative value both for binary reaction and for breakup reaction of deuteron. The reactions with excitation of levels of a nucleus ^{13}C have negative value as well.

The value of the tensor analyzing power T_{20} for $\vec{d}d \to pdn$ reaction practically coincides with the T_{20} value for $\vec{d}d \to ppnn$ reaction.

R&D of New Fast Gas Detectors at VBLHE

Two new fast MWPCs with pad readout and three-stage GEM detector with strip readout have been tested on the beam at GSI in February 2006 with Ar-CO_2 and Xe-CO_2 gas mixtures. During the analysis it was shown that efficiency and gain of this 2D detectors have not changed up to the intensity ~ 200 kHz/cm^2. New Front End ASIC Electronics was used for testing MWPC and GEM detectors. A new two-stage GEM-based detector with strip readout (pitch 0.25 and 0.5 mm) has been developed and tested in laboratory conditions, a spatial resolution ~ 100 μkm was achieved.

Applied Research

In the framework of the MARUSYA collaboration a system of transparent profilometers for dynamic diagnostics of the beam of the cyclotron at the Alpha complex (TRACKPORE TECHNOLOGY, Dubna) was developed, manufactured and put into operation. Using this system the dynamic spectra of film irradiation were studied. The methods of systematic analysis of various irradiation regimes and data certification were developed and tested.

The other results obtained at VBLHE in 2006 are published in [21–50].

REFERENCES

1. The BECQUEREL Project, web-site http://becquerel.jinr.ru/
2. *Andreeva N. P. et al.* Clustering in Light Nuclei in Fragmentation above 1 A·GeV // Eur. Phys. J. A. 2006. V. 27, s01. P. 295–300.
3. *Zarubin P. I., Artemenkov D. A., Orlova G. I.* Dissociation of Relativistic Nuclei in Peripheral Interactions in Nuclear Track Emulsion // Nuclear Science and Safety in Europe / Eds. T. Cechik et al. Springer, 2006. P. 189-200; nucl-ex/0604007.
4. *Artemenkov D. A. et al.* // Proc. of XXV Rila Workshop on Nuclear Theory. Sofia: Heron Press, 2006. P. 139–147.
5. *Artemenkov D. A. et al.* nucl-ex/0610023.
6. *Shchedrina T. V. et al.* // Phys. At. Nucl. 2007 (in press); nucl-ex/0610022.
7. *Artemenkov D. A. et al.* // Phys. At. Nucl. 2007 (in press); nucl-ex/0610018.
8. *Peresadko N. G. et al.* // Phys. At. Nucl. 2007 (in press); nucl-ex/0610014.
9. *Stanoeva R. et al.* // Phys. At. Nucl. 2007 (in press); nucl-ex/0610013.
10. *Karnaukhov V. A.* // Phys. Part. Nucl. 2006. V. 37, No. 2. P. 165–193.
11. *Karnaukhov V. A. et al.* // Phys. At. Nucl. 2006. V. 69, No. 7. P. 1142–1149.
12. *Avdeyev S. A. et al.* nucl-ex/0603001, 2006.
13. *Karnaukhov V. A. et al.* // Nucl. Phys. A. 2006. V. 780. P. 91–99.
14. *Adischev Yu. N. et al.* First Observation of Parametric X-rays Produced by Moderate Relativistic Protons and Carbon Nuclei in Si Crystals // Nucl. Instr. Meth. Phys. Res. B. 2006. V. 252. P. 111–117.
15. ALICE Physics Performance Report // J. Phys. G: Nucl. Part. Phys. 2005. V. 30. P. 1517–1763.
16. ALICE TRD, Technical Design Report. CERN/LHCC 2001-021.
17. *Lippmann C. et al.* The ALICE Transition Radiation Detector // Proc. of the SNIC Conference, SLAC, April 3–6, 2006.
18. ALICE Forges Ahead with Detector Installation // CERN Courier. 2006. V. 46, No. 10. P. 6.
19. *Agakichiev G. et al.* Dielectron Production in $^{12}\mathrm{C}+{}^{12}\mathrm{C}$ Collisions at 2 A·GeV with the HADES Spectrometer // Phys. Rev. Lett. 2007. V. 98. P. 052302.
20. Physik der Superlative, die 6 imposantesten Experimente // Bild der Wissenschaft magazin. 2006. No. 11.
21. *Malakhov A. I. et al.* Relativistic Nuclear Physics at the Joint Institute for Nuclear Research. JINR Preprint P1-2006-93. Dubna, 2006;
    Malakhov A. I. Asymptotic Regimes in Relativistic Nuclear Physics and Particle Physics // Proc. of the 8th Intern. Workshop «Relativistic Nuclear Physics: from Hundreds of MeV to TeV», Dubna, May 23–28, 2005. Dubna, 2006. P. 44–46.
22. *Karachuk J.* Invariant Properties of Pion Clusters in Different Nuclear Reactions // Proc. of the 8th Intern. Workshop «Relativistic Nuclear Physics: from Hundreds of MeV to TeV», Dubna, May 23–28, 2005. Dubna, 2006. P. 67–72.
23. *Azhgirey L. S. et al.* Relativistic Deuteron Structure from Data on the Fragmentation of Polarized Deuterons // Proc. of the 8th Intern. Workshop «Relativistic Nuclear Physics: from Hundreds of MeV to TeV», Dubna, May 23–28, 2005. Dubna, 2006. P. 92–99.
24. *Shimansky S. S.* Cumulative Processes // Proc. of the 8th Intern. Workshop «Relativistic Nuclear Physics: from Hundreds of MeV to TeV», Dubna, May 23–28, 2005. Dubna, 2006. P. 297–305.
25. *Ilic J. V., Skoro G. P., Tokarev M. V.* Jet Energy Density in Hadron–Hadron Collisions at High Energies // Part. Nucl., Lett. 2006. V. 3, No. 2(131). P. 43–52.
26. *Aslanyan P. Zh., Emelyanenko V. N., Rikhvitzkaya G. G.* Exotic Narrow Resonance Searches in the Systems ΛK_s^0 // Part. Nucl., Lett. 2006. V. 3, No. 5(134). P. 99–104.
27. *Aslanyan P.* // Proc. XVIII ISHEPP, Dubna, Sept. 25–30, 2006; Spin'06, Oct. 2–7, 2006, Kyoto, Japan.
28. *Alt C. et al. (NA49 Collab.).* Energy and Centrality Dependence of Antiproton and Proton Production and the Antilambda/Antiproton Ratio in Pb + Pb Collisions between 20 A·GeV and 158 A·GeV // Phys. Rev. C. 2006. V. 73. P. 044910.
29. *Alt C. et al. (NA49 Collab.).* Upper Limit of D^0 Production in Central Pb + Pb Collisions at 158 GeV // Phys. Rev. C. 2006. V. 73. P. 034910.
30. *Alt C. et al. (NA49 Collab.).* Inclusive Production of Charged Pions in $p+p$ Collisions at 158 GeV/c Beam Momentum // Eur. Phys. J. C. 2006. V. 45. P. 343–381.
31. *Adler S. S. et al.* Improved Measurement of Double Helicity Asymmetry in Inclusive Midrapidity π^0 Production for Polarized $p+p$ Collisions at $\sqrt{s}=200$ GeV // Phys. Rev. D. 2006. V. 73. P. 091102(R).
32. *Adler S. S. et al.* Azimuthal Angle Correlations for Rapidity Separated Hadron Pairs in $d+\mathrm{Au}$ Collisions at $\sqrt{S_{NN}}=200$ GeV // Phys. Rev. Lett. 2006. V. 96. P. 222301.
33. *Adler S. S. et al.* Nuclear Modification of Electron Spectra and Implications for Heavy Quark Energy Loss in Au + Au Collisions at $\sqrt{S_{NN}}=200$ GeV // Ibid. P. 032301.
34. *Adler S. S. et al.* Common Suppression Pattern of η and π^0 Mesons at High Transverse Momentum in Au + Au Collisions at $\sqrt{S_{NN}}=200$ GeV // Ibid. P. 202301.
35. *Adler S. S. et al.* Measurement of Identified π^0 and Inclusive Photon Second-Harmonic Parameter ν_2 and Implications for Direct Photon Production in $\sqrt{S_{NN}}=200$ GeV Au + Au // Ibid. P. 032302.
36. *Tokarev M. V.* z-Scaling at RHIC // Part. Nucl., Lett. 2006. V. 3, No. 1(130). P. 17–30.
37. *Zborovsky I., Tokarev M.* Generalized z-Scaling in Proton–Proton Collisions at High Energies. JINR Preprint E2-2006-34. Dubna, 2006.
38. *Kosmachev O. S.* Lorentz Group Representation and Classification of Stable Leptons. JINR Preprint P2-2006-6. Dubna, 2006.

39. *Adams J. et al.* Identified Hadron Spectra at Large Transverse Momentum in $p + p$ and $d + \mathrm{Au}$ Collisions at $\sqrt{S_{NN}} = 200$ GeV // Phys. Lett. B. 2006. V. 637, issue 3. P. 161–169.
40. *Krizek F. et al.* The Study of Spallation Reactions, Neutron Production and Transport in a Thick Lead Target and a Uranium Blanket during 1.5 GeV Proton Irradiation // Czechoslovak J. Phys. 2006. V. 56, No. 3. P. 243–252.
41. *Bystritsky V. M. et al.* Portable Neutron Generator with 9-Section Silicon α-Detector. JINR Preprint E13-2006-36. Dubna, 2006.
42. *Anishchenko N. G. et al.* Superconducting Magnetic System with a Cryocooler for the Ion Source DECRIS-SC // Part. Nucl., Lett. 2006. V. 3, No. 1(130). P. 45–62.
43. *Kuznetsov A. A. et al.* Properties of the Hadronic Jets in $\pi^- + p$ and $\pi^- + \mathrm{C}$ Interactions at 40 GeV/c // Ibid. No. 2 (131). P. 53–72.
44. *Yurevich V. I. et al.* Investigation of Neutron Emission at Interaction of Relativistic Protons and Deuterons with Lead Targets // Ibid. No. 3(132). P. 49–72.
45. *Artemov A. S.* Calculation of Internal Targets and Schematic Diagram of Compact Devices for Continuous Visualization of a Synchrotron Beams, as Exemplified by the Nuclotron // Ibid. No. 4(133). P. 48–67.
46. *Artemov A. S. et al.* Schematic Diagram and Calculation of Magnetic Electron Analyzer for Investigations in the Field of Relativistic Atomic Physics at Internal Targets of the Nuclotron. JINR Preprint P13-2006-64. Dubna, 2006; submitted to «Part. Nucl., Lett.».
47. *Troyan Yu. et al.* The Study of the Low-Mass Scalar σ_0-meson at Intermediate Energies // Proc. of the 8th Intern. Workshop «Relativistic Nuclear Physics: from Hundreds of MeV to TeV», Dubna, May 23–28, 2005. Dubna, 2006. P. 136–147.
48. *Vokal S., Lehocka S., Orlova G. I.* Dense Groups of Particles in High Energy Nuclear Interactions of Lead and Gold Nuclei in Nuclear Emulsion // Proc. of the 8th Intern. Workshop «Relativistic Nuclear Physics: from Hundreds of MeV to TeV», Dubna, May 23–28, 2005. Dubna, 2006. P. 194–202.
49. *Zaitsev L.N. et al.* Radiation Resistance of Electric Insulation Compound of Superconducting Magnets of Accelerators. JINR Preprint P14-2006-43. Dubna, 2006.
50. *Yashemi-Nezhad S. R. et al.* Calibration of Track Detectors for Fission Rate Determination: an Experimental and Theoretical Study. JINR Preprint E1-2006-54. Dubna, 2006.